A&A 620, A54 (2018)
https://doi.org/10.1051/0004-6361/201833753

Astronomy & Astrophysics

Using non-solar-scaled opacities to derive stellar parameters

Toward high-precision parameters and abundances

C. Saffe[1,2,5], M. Flores[1,2,5], P. Miquelarena[2], F. M. López[1,2,5], M. Jaque Arancibia[1,4,5], A. Collado[1,2,5], E. Jofré[3,5], and R. Petrucci[3,5]

[1] Instituto de Ciencias Astronómicas, de la Tierra y del Espacio (ICATE-CONICET), C.C 467, 5400, San Juan, Argentina
e-mail: saffe.carlos@gmail.com
[2] Universidad Nacional de San Juan (UNSJ), Facultad de Ciencias Exactas, Físicas y Naturales (FCEFN), San Juan, Argentina
[3] Observatorio Astronómico de Córdoba (OAC), Laprida 854, X5000BGR, Córdoba, Argentina
[4] Departamento de Física y Astronomía, Universidad de La Serena, Av. Cisternas 1200. 1720236, La Serena, Chile
[5] Consejo Nacional de Investigaciones Científicas y Técnicas (CONICET), Argentina

Received 1 July 2018 / Accepted 24 September 2018

ABSTRACT

Aims. In an effort to improve spectroscopic methods of stellar parameters determination, we implemented non-solar-scaled opacities in a simultaneous derivation of fundamental parameters and abundances. We wanted to compare the results with the usual solar-scaled method using a sample of solar-type and evolved stars.
Methods. We carried out a high-precision determination of stellar parameters and abundances by applying non-solar-scaled opacities and model atmospheres. Our sample is composed of 20 stars, including main sequence and evolved objects. The stellar parameters were determined by imposing ionization and excitation equilibrium of Fe lines, with an updated version of the FUNDPAR program, together with plane-parallel ATLAS12 model atmospheres and the MOOG code. Opacities for an arbitrary composition and $v_{\rm micro}$ were calculated through the opacity sampling (OS) method. We used solar-scaled models in the first step, and then continued the process, but scaled to the abundance values found in the previous step (i.e. non-solar-scaled). The process finishes when the stellar parameters of one step are the same as in the previous step, i.e. we use a doubly iterated method.
Results. We obtained a small difference in stellar parameters derived with non-solar-scaled opacities compared to classical solar-scaled models. The differences in $T_{\rm eff}$, log g, and [Fe/H] amount to 26 K, 0.05 dex, and 0.020 dex for the stars in our sample. These differences can be considered the first estimation of the error due to the use of classical solar-scaled opacities to derive stellar parameters with solar-type and evolved stars. We note that some chemical species could also show an individual variation greater than those of the [Fe/H] (up to ∼0.03 dex) and varying from one species to another, obtaining a chemical pattern difference between the two methods. This means that condensation temperature $T_{\rm c}$ trends could also present a variation. We include an example showing that using non-solar-scaled opacities, the solution found with the classical solar-scaled method indeed cannot always verify the excitation and ionization balance conditions required for a model atmosphere. We discuss in the text the significance of the differences obtained when using solar-scaled versus non-solar-scaled methods.
Conclusions. We consider that the use of the non-solar-scaled opacities is not mandatory in every statistical study with large samples of stars. However, for those high-precision works whose results depend on the mutual comparison of different chemical species (such as the analysis of condensation temperature $T_{\rm c}$ trends), we consider its application to be worthwhile. To date, this is probably one of the most precise spectroscopic methods for stellar parameter derivation.

Key words. stars: fundamental parameters – stars: abundances – stars: atmospheres

1. Introduction

The discovery of the first exoplanets orbiting the pulsar PSR1257+12 (Wolszczan & Frail 1992) and the solar-type star 51 Peg (Mayor & Queloz 1995) gave rise to a number of works which were strong motivations to increase the precision of both photometry and spectroscopy techniques. This continuous effort allowed the discovery of new planets and its subsequent analysis. For instance, radial-velocity measurements were improved to a precision of a few m s^{-1} or less (e.g. Lo Curto et al. 2015; Fischer et al. 2016), while the *Kepler* photometry could reach <1 millimag for a 12th mag star[1]. The derivation of detailed chemical abundances followed a similar path. For example, the use of the differential technique applied to physically similar stars, allowed the dispersion in [Fe/H] to be significantly reduced to values close to or lower than ∼0.01 dex (e.g. Desidera et al. 2004; Meléndez et al. 2009; Ramírez et al. 2011; Saffe et al. 2015, 2016, 2017). These high-precision values are needed, for example, to detect a possible chemical signature of planet formation (e.g. Meléndez et al. 2009; Saffe et al. 2016) and are also required by the chemical tagging technique. It is crucial to pursue the maximum possible precision in the derivation of stellar parameters and chemical patterns.

Several works use a two-step method of abundance determination in order to determine the chemical composition of solar-type stars. This was applied, for instance, in the study of stellar galactic populations (e.g. Adibekyan et al. 2012, 2013, 2014, 2016; Delgado Mena et al. 2017), metallicity trends in stars with and without planets (e.g. Sousa et al. 2008, 2011a,b;

[1] https://keplergo.arc.nasa.gov/pages/photometric-performance.html

Adibekyan et al. 2012) and the possible signature of terrestrial planets (e.g. González Hernández et al. 2010, 2013; Adibekyan et al. 2014). These works are not an exhaustive list, but exemplify a number of important studies and trends. Briefly, in the first step the fundamental parameters are determined by imposing excitation and ionization equilibrium of Fe I and Fe II lines. The model atmosphere which satisfies these conditions is usually interpolated or calculated by assuming both solar-scaled opacities and abundances. Once the stellar parameters are fixed, in the second step the chemical abundances are determined by using equivalent widths or spectral synthesis, depending on the possible presence of blends and other effects such as hyperfine structure (HFS). The process normally finishes here, resulting in a chemical pattern that is not exactly solar-scaled, as supposed in the first step. Notably, even reaching a perfect match between synthetic and observed spectra, this inconsistency could lead to an incorrect determination of stellar parameters and abundances. In addition, this issue is generally unaccounted for in the total error estimation of most literature works.

Then, in an effort to improve the precision of the results, the appropriate calculation of the model atmospheres should include the previous derivation of opacities obtained for a specific abundance pattern beyond the classical solar-scaled values. We wonder if it is possible to implement such a method in the calculation of stellar parameters in a practical way. What is the difference in the stellar parameters obtained with this procedure and the classical solar-scaled methods? How many iteration steps are necessary to properly derive the stellar parameters? Can this effect introduce a statistical bias in studies of large samples? Do we expect a null difference in metallicity between very similar components of binary stars? These important questions are the motivation of the present work.

This work is organized as follows. In Sect. 2, we describe the sample and data reduction, while in Sect. 3 we explain the calculation of opacities and models. Finally, we present the discussion and conclusions in Sects. 4 and 5.

2. Sample of spectra

As previously mentioned, the detection of the possible chemical signature of planet formation requires a very high precision in stellar parameters. These studies are usually performed on solar-type main-sequence stars (e.g. Tucci Maia et al. 2014; Saffe et al. 2015, 2016). We start by choosing ten objects of this type for our sample. In order to study the possible differences between solar-scaled and non-solar-scaled methods in other types of stars, we also included in our sample 10 giant stars (see Table 1). Then, the final sample is composed of 20 stars with $T_{\rm eff}$ in the range 4131–8333 K and log g in the range 1.62–4.64 dex. Their metallicities range from −0.43 to +0.27 dex, including objects with values lower and higher than that of the Sun, and likely including a number of different chemical mixtures. Six stars in our sample belong to binary systems previously studied in the literature (Saffe et al. 2015, 2016, 2017; hereafter SA15, SA16, SA17). In particular, the binary systems were selected for the high degree of physical similarity between their components, which allow us to test the possible variation in the stellar parameters (scaled versus non-solar-scaled) depending on the chemical pattern, which is roughly similar for the two stars in each binary system.

For the stars studied in this work, Table 1 presents the corresponding spectrograph, resolving power, signal-to-noise ratio, and object used as a proxy for the Sun spectra. We reduced the data by using the reduction package MAKEE 3 with HIRES spectra[2], the Data Reduction Software (DRS) pipeline with HARPS data[3], and the OPERA 5 (Martioli et al. 2012) software with GRACES spectra. The continuum normalization and other operations (such as Doppler correction and combining spectra) were performed using the Image Reduction and Analysis Facility (IRAF)[4].

Table 1. Sample of spectra used in this work.

Stars	Spectrograph	R	S/N	Sun spectra
Main-sequence stars				
HD 80606 + HD 80607	HIRES	67 000	~330	Iris
ζ^1 Ret + ζ^2 Ret	HARPS	110 000	~300	Ganymede
HAT-P-4 + TYC 2567-744-1	GRACES	67 500	~400	Moon
HD 19994	HARPS	115 000	~390	Ganymede
HD 221287	HARPS	115 000	~130	Ganymede
HD 96568	HARPS	115 000	~350	Ganymede
HD 128898	HARPS	115 000	~340	Ganymede
Evolved stars				
HD 2114	HARPS	115 000	~180	Ganymede
HD 10761	HARPS	115 000	~195	Ganymede
HD 28305	HARPS	115 000	~180	Ganymede
HD 32887	HARPS	115 000	~245	Ganymede
HD 43023	HARPS	115 000	~275	Ganymede
HD 50778	HARPS	115 000	~140	Ganymede
HD 85444	HARPS	115 000	~225	Ganymede
HD 109379	HARPS	115 000	~335	Ganymede
HD 115659	HARPS	115 000	~310	Ganymede
HD 152334	HARPS	115 000	~195	Ganymede

3. Calculating non-solar-scaled opacities and models

Within the suite of Kurucz's programs for model atmosphere calculation, a non-solar-scaled model can be calculated in two different ways. The first option consists in the previous calculation of an opacity distribution function (ODF), which depends on the abundances and microturbulence velocity $v_{\rm micro}$, and which is then used as input for an ATLAS9 model atmosphere (see e.g. Kurucz et al. 1974; Castelli 2005b). The second option consists directly in the calculation of an ATLAS12 model atmosphere, which calculates internally the opacities through the opacity sampling (OS) method (see e.g. Peytremann 1974; Kurucz 1992; Castelli 2005a).

We briefly describe both options here. ODF functions used by ATLAS9 are tables which describe the dependence of the line absorption coefficient l_ν as a function of the frequency ν, calculated for a given pair $T_{\rm gas}$ and $P_{\rm gas}$ (see e.g. Kurucz et al. 1974; Castelli 2005b). Different sets of ODFs are derived for fixed abundances (usually solar-scaled and some α-enhanced models) and fixed $v_{\rm micro}$ (see e.g. Castelli & Kurucz 2003; Coelho 2014). Strictly speaking, the calculation of an ATLAS9 model atmosphere for a specific composition and $v_{\rm micro}$ should include the

[2] http://www.astro.caltech.edu/ tb/makee/
[3] https://www.eso.org/sci/facilities/lasilla/instruments/harps/doc.html
[4] IRAF is distributed by the National Optical Astronomical Observatories, which is operated by the Association of Universities for Research in Astronomy, Inc., under a cooperative agreement with the National Science Foundation.

previous calculation of the ODF for the corresponding values using the DFSYNTHE program (see e.g. Castelli 2005b). Otherwise, the numerical abundances derived for the ions during the actual model calculation at a given gas state ($T_{\rm gas}$ and $P_{\rm gas}$) will differ from those calculated during the ODF computation. On the other hand, it is also possible to derive an ATLAS12 model atmosphere in which the OS method determines the opacity for given abundances and $v_{\rm micro}$. This is an important detail given that the correct derivation of a model atmosphere for an arbitrary chemical pattern should include the specific opacities and not only a mere change in the abundances used. The longer time required for the calculation of an ATLAS12 model compared to ATLAS9 is not a problem today; the operation finishes after only a few minutes. A complete ATLAS12 version for *gfortran* is available at the Fiorella Castelli's webpage[5], while for DFSYNTHE there is only an ifort (intel) version. Thus, we used ATLAS12 for the calculation of a non-solar-scaled model atmosphere.

Usually, ATLAS12 model atmospheres are used when, for example, the chemical composition of the stars present α-elements patterns that do not follow solar-scaled or α-enhanced models, or for early-type stars where diffusion effects change significantly their superficial composition (see e.g. Sbordone et al. 2005; Mucciarelli et al. 2012). For this work, we used non-solar-scaled opacities (calculated by ATLAS12) for the simultaneous derivation of both stellar parameters and abundances, as we explain in the next section.

4. Stellar parameters and chemical abundance analysis

We started by measuring the equivalent widths of Fe I and Fe II lines in the spectra using the IRAF task *splot*, and then continued with other chemical species. The lines list and relevant laboratory data (such as excitation potential and oscillator strengths) are similar to those used in previous works (SA15, SA16). However, we note that the exact values are not very relevant here, given the differential technique applied in this case.

The first estimation of the stellar parameters ($T_{\rm eff}$, log g, [Fe/H], $v_{\rm micro}$) uses an iterative process within the FUNDPAR program (Saffe 2011), searching for a model atmosphere which satisfies the excitation and ionization balance of Fe I and Fe II lines. This code was improved in order to use the program MOOG (Sneden 1973) together with ATLAS12 opacities and model atmospheres (Kurucz 1993). The procedure uses explicitly calculated (i.e. non-interpolated) plane-parallel local thermodynamic equilibrium (LTE) Kurucz model atmospheres with ATLAS12, which includes the internal calculation of the line opacities through the OS method. Two runs of ATLAS12 are used (see e.g. Castelli 2005a): the first for a preselection of important lines (for the given stellar parameters and abundances) and the second for the final calculation of the model structure. In both runs, we explicitly use a specific chemical pattern.

The models are calculated with overshooting in order to facilitate the comparison with previous works (e.g. SA15, SA16, SA17). However, we caution that this modification of the mixing-length theory is suitable for the Sun, but not necessarily for other stars (Castelli et al. 1997). The overshooting produces a thermal structure that disagrees with that obtained from hydrodynamical simulations, being magnified for low metallicity and disappears for solar metallicity (see Fig. C.1 in Bonifacio et al. 2009). We adopted the layer 36 in the atmosphere where numerical results related with the Schwarzschild criterion can be assumed as reliable for models with $T_{\rm eff} > 4000$ K (Castelli 2005a).

We applied in this work the full differential technique: we considered the individual line-by-line differences between each star and the Sun, which is used as the reference star. The object used as a proxy for the solar spectra (in reflected light) is listed in the last column of Table 1. We first determined absolute abundances for the Sun using 5777 K for $T_{\rm eff}$, 4.44 dex for log g, and an initial $v_{\rm micro}$ of 1.0 km s^{-1}. Then, we estimated $v_{\rm micro}$ for the Sun with the usual method of requiring zero slope in the absolute abundances of Fe I lines versus reduced equivalent widths and obtained a final $v_{\rm micro}$ of 0.91 km s^{-1}. We note, however, that the exact values are not crucial for our strictly differential study (see e.g. Bedell et al. 2014; SA15). The next step is the derivation of stellar parameters for all stars in our sample using the Sun as reference (i.e. star – Sun). We note that this line-by-line method is applied both in the derivation of stellar parameters and in the chemical abundances (i.e. the "full" differential technique), which increases the precision of stellar parameters (e.g. SA15, SA16).

In the first FUNDPAR iteration we used solar-scaled models for an initial estimation of stellar parameters. Then a starting set of chemical abundances were determined using equivalent widths and spectral synthesis. In the next step, the iterative process within FUNDPAR was restarted, but scaled using the last set of abundances instead of the initial solar-scaled values. At this point, we took advantage of the ATLAS12 opacities and models calculated on the fly at the request of FUNDPAR for an arbitrary chemical composition and $v_{\rm micro}$. We note that the possibility to scale to an arbitrary chemical pattern (through an ABUNDANCE SCALE control card) was implemented by Dr. Fiorella Castelli and is not available in the original Kurucz code (Castelli 2005a). In this way, new stellar parameters and abundances are successively derived, finishing the process consistently when the stellar parameters are the same as the previous step. The process described here is then a doubly iterated process, with the FUNDPAR iteration contained within a larger (abundance-scaled) iteration. The classical solar-scaled results correspond to the values derived in the first step of this new scheme.

We computed the individual abundances for the following elements: C I, O I, Na I, Mg I, Al I, Si I, S I, Ca I, Sc I, Sc II, Ti I, Ti II, V I, Cr I, Cr II, Mn I, Fe I, Fe II, Co I, Ni I, Cu I, Sr I, Y II, and Ba II. The HFS splitting was considered for V I, Mn I, Co I, Cu I, and Ba II by adopting the HFS constants of Kurucz & Bell (1995) and performing spectral synthesis with the program MOOG (Sneden 1973) for these species. We used exactly the same lines (laboratory data and equivalent widths) for iron and for all chemical species when deriving stellar parameters and abundances with the two methods (scaled and non-solar-scaled).

5. Results and discussion

In Fig. 1 we show two examples of chemical pattern derived using the classical solar-scaled method (red) and the doubly iterated method (blue) for the stars HAT-P-4 and HD 80606 (upper and lower figures). For each star the lower panel shows the abundance differences between the methods. We note that some of these differences are notably larger than the ~0.01 dex of the [Fe/H] (e.g. for La, Ce, Nd, Sm, and Dy in HAT-P-4), reaching up to ~0.03 dex. Other species show even a contrary or negative difference (e.g. C and O in the same panel). This behavior of the different chemical elements is also seen in other

[5] http://wwwuser.oats.inaf.it/castelli/

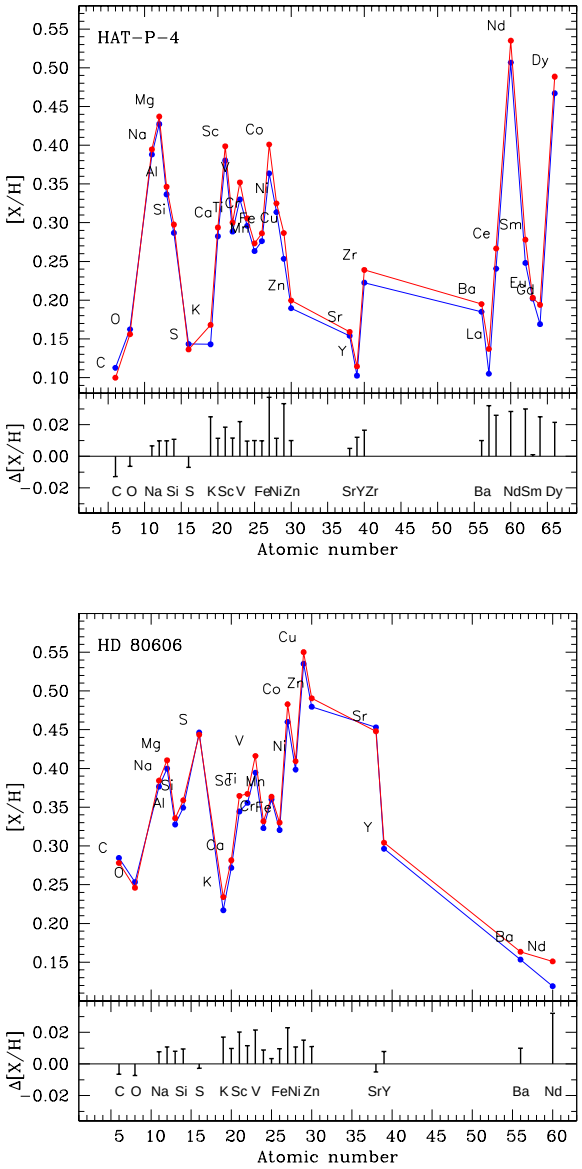

Fig. 1. Chemical pattern derived using the classical solar-scaled method (red) and the new method (blue). The two small lower panels show the abundance differences between the methods, i.e. a chemical pattern difference. The upper and lower figures correspond to the stars HAT-P-4 and HD 80606.

stars (see e.g. HD 80606, lower panel of Fig. 1). In principle, we can consider these differences as a "chemical pattern difference" derived from the use of one method or another, which is to our knowledge shown for the first time in this work. However, we caution that this pattern difference could change from star to star, depending on the specific opacities (composition) and fundamental parameters.

We present in Table 2 the final stellar parameters derived using the new scheme proposed here, together with the individual errors shown as $T_{\rm eff} \pm \xi_{T{\rm eff}}$, $\log g \pm \xi_{\log g}$, etc. The errors were derived following the same procedure used in previous works, taking into account independent and covariance terms in the error propagation (see e.g. Sect. 3 of SA15 for more details). In addition, in parentheses we show the difference between the two procedures (new method − solar-scaled method). The greater differences in $T_{\rm eff}$, $\log g$, [Fe/H], and $\upsilon_{\rm micro}$ amount to (absolute values) 26 K, 0.05 dex, 0.020 dex, and 0.05 km s^{-1}. However, it is interesting to separate the results of main-sequence and giant stars, which seem to show a slightly different behaviour. For instance, there is no evolved star with a $T_{\rm eff}$ difference greater than ∼10 K, while many main-sequence objects are above this value. A similar effect is seen in the average $\upsilon_{\rm micro}$ differences: there is no giant star with a $\upsilon_{\rm micro}$ difference greater than 0.02 km s^{-1}, while many main-sequence objects are above this value. On the other hand, there is no clear difference in the average difference values of main-sequence and giant stars when comparing $\log g$ and [Fe/H] values. We also note that the greater difference in $T_{\rm eff}$ corresponds to a main-sequence star (HAT-P-4 with 26 K), while the greater difference in [Fe/H] corresponds to an evolved object (HD 32887 with 0.020 dex).

In general, the differences obtained between the solar-scaled method and the new method are comparable to the individual dispersions of the values of the stellar parameters. In particular, we note that some [Fe/H] differences are larger than or similar to the dispersions. For the other three stellar parameters ($T_{\rm eff}$, $\log g$, and $\upsilon_{\rm micro}$) the differences are usually smaller than the individual dispersions. This means that using the non-solar-scaled method is not necessarily mandatory for every determination of the stellar parameters. However, there are some physical processes that claim a higher precision in order to be well described. We specifically discuss the significance of these differences in Sect. 5.1.

Given the differences found in stellar parameters shown in Table 2, we should expect small differences (although not identical) in the model structures derived using the two methods. We present in Fig. 2 four examples comparing solar-scaled (blue dashed lines) and non-solar-scaled (red continuous lines) ATLAS12 model atmospheres. This figure include two main-sequence stars (HD 19994, HAT-P-4) and two giant stars (HD 32887, HD 115659). For each star, we show the temperature T and pressure P as a function of the Rosseland depth $\tau_{\rm Ross}$, as derived from the ATLAS12 model atmospheres. We included intentionally the star HD 19994 in these plots, which shows one of the smallest differences in stellar parameters when derived using both methods (see Table 2). The temperature distributions using the two methods are similar in general. However, the small insets present a zoom of the temperature distribution, showing indeed that the distributions are not identical: HD 19994 shows a slightly higher T for the solar-scaled method than for the new method, while the other three stars shows a lower T for the solar-scaled method, i.e. the opposite difference. This corresponds directly to the slightly higher and lower $T_{\rm eff}$, respectively, obtained with the two methods for these stars (see Table 2). In other words, a slightly higher T distribution corresponds to a slightly higher $T_{\rm eff}$. In the same Fig. 2, we also see that the pressure distributions show a more noticeable difference when calculated using the two methods. In particular, the smallest difference corresponds in this example to HD 19994, showing one of the smallest differences in parameters in the Table 2. We note that the small differences found between the models shown in Fig. 2 include the range $-1 < \log \tau_{\rm Ross} < 1$ where we expect that most nonsaturated spectral lines should form. Then, the plots in Fig. 2 show that the structure of the model atmospheres, as expected, are similar but not identical (even for stars such as HD 19994), and the differences correspond to the differences found in the stellar parameters shown in Table 2.

We also performed the following experiment. Using non-solar-scaled opacities, we derived the abundances of Fe I and Fe II, but applied the solution found with the solar-scaled method. We present in Fig. 3 the corresponding results, showing the iron abundance versus excitation potential and iron

Table 2. Stellar parameters derived using the new doubly iterated method.

Star	$T_{\rm eff}$ (K)	log g (dex)	[Fe/H] (dex)	$v_{\rm micro}$ (km s^{-1})	$s_{\rm classic}$ (10^{-5} dex K^{-1})	$s_{\rm new}$ (10^{-5} dex K^{-1})
Main-sequence stars						
HAT-P-4	6064 ± 35 (+26)	4.34 ± 0.08 (−0.01)	+0.220 ± 0.005 (+0.009)	1.30 ± 0.09 (+0.04)	+12.37 ± 1.53	+13.70 ± 1.50
TYC 2567-744-1	6055 ± 37 (+15)	4.37 ± 0.07 (−0.01)	+0.104 ± 0.006 (+0.012)	1.22 ± 0.10 (+0.02)	+3.98 ± 0.81	+5.29 ± 0.95
HD 80606	5579 ± 28 (+25)	4.31 ± 0.10 (+0.02)	+0.268 ± 0.002 (+0.009)	0.91 ± 0.07 (+0.04)	+2.38 ± 0.94	+4.17 ± 0.85
HD 80607	5505 ± 34 (+16)	4.29 ± 0.11 (+0.01)	+0.249 ± 0.004 (+0.006)	0.88 ± 0.09 (+0.03)	+3.23 ± 0.64	+4.30 ± 0.55
ζ^1 Ret	5725 ± 29 (+11)	4.50 ± 0.05 (+0.00)	−0.251 ± 0.003 (+0.010)	0.94 ± 0.05 (+0.05)	+2.67 ± 1.26	+2.81 ± 1.21
ζ^2 Ret	5874 ± 27 (+13)	4.52 ± 0.07 (−0.01)	−0.270 ± 0.004 (+0.009)	1.08 ± 0.06 (+0.05)	−2.31 ± 1.37	−0.84 ± 1.34
HD 19994	6245 ± 39 (−4)	4.42 ± 0.15 (+0.00)	+0.228 ± 0.010 (−0.001)	1.38 ± 0.11 (−0.01)	−2.82 ± 1.37	−3.51 ± 1.37
HD 221287	6340 ± 40 (−6)	4.63 ± 0.13 (+0.01)	+0.007 ± 0.010 (−0.001)	1.28 ± 0.12 (−0.01)	+7.60 ± 1.48	+7.47 ± 1.47
HD 96568	8333 ± 39 (−14)	3.59 ± 0.09 (+0.04)	−0.081 ± 0.005 (+0.010)	1.54 ± 0.08 (+0.02)	+6.56 ± 4.77	+6.40 ± 4.77
HD 128898	8035 ± 27 (−8)	4.64 ± 0.09 (+0.02)	+0.099 ± 0.008 (+0.008)	1.59 ± 0.11 (−0.03)	+7.99 ± 4.82	+6.59 ± 4.84
Evolved stars						
HD 2114	5308 ± 35 (−8)	2.87 ± 0.12 (−0.03)	−0.047 ± 0.010 (+0.000)	1.86 ± 0.10 (−0.01)	+3.06 ± 1.87	+3.03 ± 1.87
HD 10761	5036 ± 32 (+8)	2.74 ± 0.10 (−0.03)	+0.018 ± 0.007 (+0.005)	1.49 ± 0.09 (+0.01)	+7.04 ± 2.50	+7.22 ± 2.46
HD 28305	5020 ± 41 (+1)	3.00 ± 0.11 (+0.01)	+0.157 ± 0.006 (+0.004)	1.72 ± 0.11 (−0.01)	+9.36 ± 2.68	+9.42 ± 2.66
HD 32887	4271 ± 39 (+6)	1.91 ± 0.12 (−0.04)	−0.169 ± 0.006 (+0.020)	1.57 ± 0.08 (+0.00)	+6.62 ± 3.10	+7.47 ± 3.10
HD 43023	5069 ± 29 (−7)	3.05 ± 0.11 (+0.01)	−0.020 ± 0.004 (−0.001)	1.25 ± 0.05 (−0.02)	+4.44 ± 1.82	+3.64 ± 1.81
HD 50778	4131 ± 39 (+7)	1.62 ± 0.16 (−0.05)	−0.431 ± 0.007 (+0.014)	1.60 ± 0.10 (+0.00)	+4.42 ± 3.08	+5.34 ± 3.10
HD 85444	5179 ± 31 (+2)	2.97 ± 0.14 (−0.01)	+0.051 ± 0.010 (+0.004)	1.47 ± 0.07 (+0.00)	+5.61 ± 2.02	+7.72 ± 2.08
HD 109379	5240 ± 36 (+5)	2.75 ± 0.15 (+0.00)	−0.003 ± 0.006 (+0.005)	1.75 ± 0.13 (+0.00)	−1.80 ± 2.35	−1.50 ± 2.35
HD 115659	5159 ± 29 (+4)	2.94 ± 0.13 (−0.02)	+0.066 ± 0.008 (+0.004)	1.49 ± 0.07 (+0.00)	+8.74 ± 2.28	+9.03 ± 2.26
HD 152334	4291 ± 37 (+5)	2.11 ± 0.12 (−0.01)	−0.072 ± 0.005 (+0.010)	1.41 ± 0.11 (−0.01)	+5.92 ± 3.04	+6.67 ± 3.56

Notes. The difference between both procedures is indicated with parentheses (as new method − solar-scaled method).

abundance versus reduced EW for the star HAT-P-4 (upper and lower panels). Filled and empty points correspond to Fe I and Fe II, while the dashed line shows a linear fit to the abundance values. It can be clearly seen from the plots that the four conditions required to find an appropriate solution for the model atmosphere (see Sect. 4) are not satisfied simultaneously. The average Fe II abundance is higher than the Fe I average (0.24 and 0.21 dex, respectively), with 8/10 Fe II lines above the Fe I average. Also, the abundances do present a slight trend with the reduced equivalent widths (lower panel). Even admitting a null slope in both panels of Fig. 3, the fact that only one condition is not verified (e.g. the ionization balance) is enough to show that the stellar parameters using the solar-scaled method were not exactly derived, and thus that a new solution could improve the previous one. This new solution will need to change the four stellar parameters, not only one, because the four mentioned conditions are not independent of each other. This task is done by the downhill simplex method within the FUNDPAR program, using non-solar-scaled opacities as explained in Sect. 4.

From Table 2, we note that four main-sequence stars show a negative difference in $T_{\rm eff}$ between the two methods (HD 19994, HD 221287, HD 96568, and HD 128898), being the stars with the highest $T_{\rm eff}$ in the main-sequence sample. We then wonder if the differences between the two methods depend only on one parameter, for example $T_{\rm eff}$. HAT-P-4 and HD 80606 both differ by ∼+25 K when using the two methods, but have a $T_{\rm eff}$ difference of ∼485 K. Also, TYC 2567-744-1 and HD 80607 differ by ∼+15 K between the two methods and have a $T_{\rm eff}$ difference of ∼550 K. Thus, we cannot adopt $T_{\rm eff}$ alone as a proxy for the differences between the two methods, although it seems to play a role. Due to the explicit calculation of the opacities for specific composition, we should expect that the differences also depend on the detailed chemical composition of each target.

We note that the differences in [Fe/H] between the methods are very similar when considering two stars in the same binary system. For instance, HD 80606 and HD 80607 present differences of +0.009 and +0.006 dex, while ζ^1 Ret and ζ^2 Ret present differences of +0.010 and +0.009 dex. This implies that the mutual difference in [Fe/H] between binary components is approximately preserved when considering two very similar stars.

The last two columns in Table 2 show the slope of abundance versus condensation temperature $T_{\rm c}$, using abundances of the classical solar-scaled method (slope $s_{\rm classic}$) and abundances of the new scheme (slope $s_{\rm new}$). Condensation temperatures were taken from the 50% $T_{\rm c}$ values derived by Lodders (2003) for a solar system gas with [Fe/H] = 0. In particular for the binary systems of Table 2, if one star presents a higher $s_{\rm classic}$ value than its binary companion, then the same star also presents a higher slope $s_{\rm new}$ in the new method. Thus, the $T_{\rm c}$ trends of previous works (SA15, SA16, SA17) are verified. However, we do not consider that this is necessarily the rule because the slopes $s_{\rm classic}$ and $s_{\rm new}$ both present small but noticeable differences between them in general, differences which are comparable to the error of the slopes, and so cannot be totally ignored.

From Table 2, the values of $s_{\rm new}$ and $s_{\rm classic}$ values are similar within their errors, showing in general smaller differences for giants than for main-sequence stars. Some slopes of the $T_{\rm c}$ trends remain almost identical (e.g. $s_{\rm new}$ and $s_{\rm classic}$ of HD 2114 are 3.03 ± 1.87 and 3.06 ± 1.87), while other $T_{\rm c}$ trends could change their original slopes by up to ∼100% of (e.g. $s_{\rm new}$ and $s_{\rm classic}$ of HD 80606 are 2.38 ± 0.94 and 4.17 ± 0.85). We note that main-sequence stars with lower $T_{\rm eff}$ seem to show higher $s_{\rm new}$ values than $s_{\rm classic}$, while stars with $T_{\rm eff}$ higher than ∼6200 K

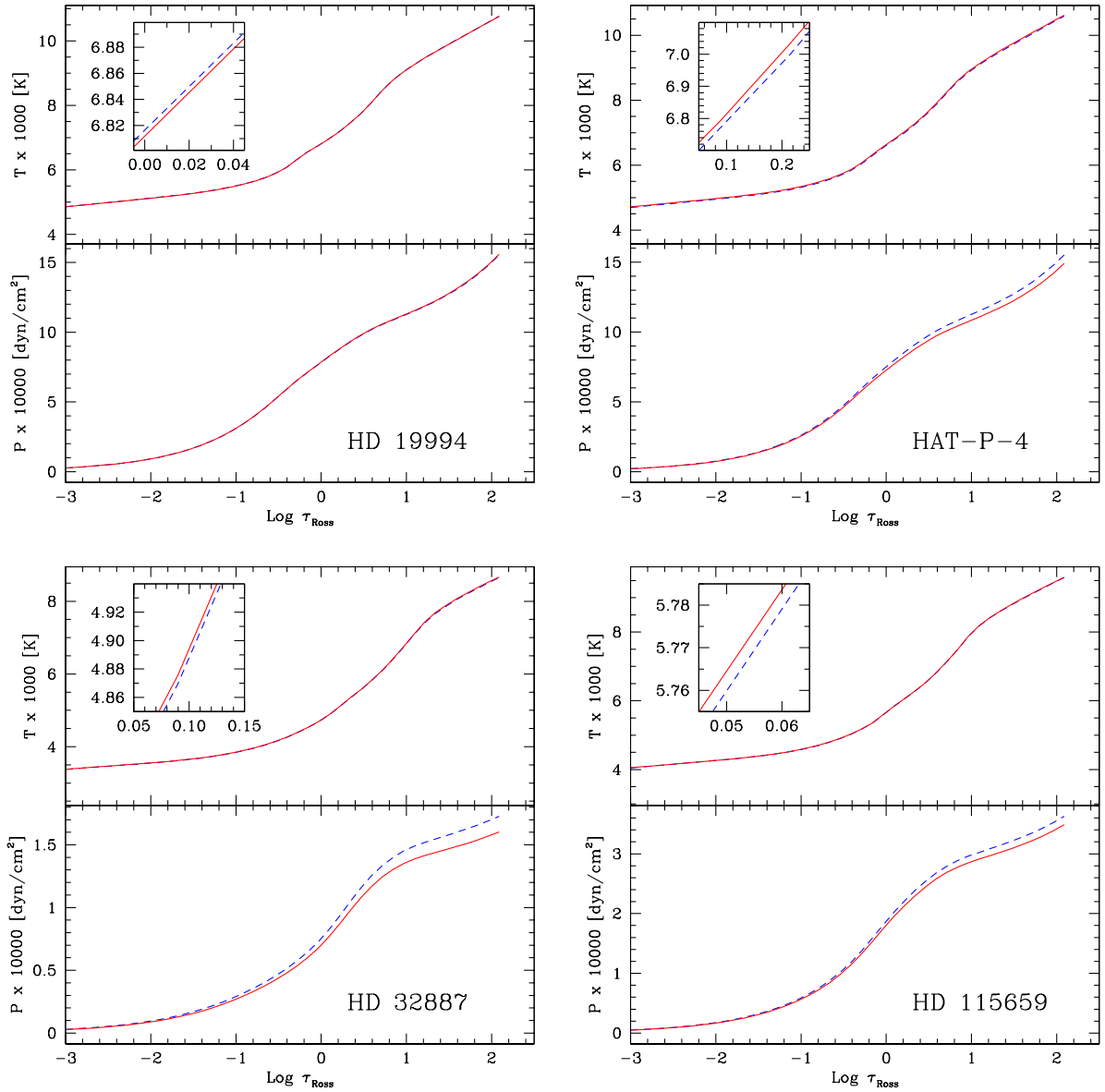

Fig. 2. Comparison of solar-scaled (blue dashed lines) vs. non-solar-scaled (red continuous lines) ATLAS12 model atmospheres. The example shows temperature and pressure distributions of four different stars (see text for details).

seem to show the opposite effect. For giant stars, those stars with $T_{\rm eff}$ lower than ∼4500 K seem to show $s_{\rm new}$ greater than $s_{\rm classic}$, while for higher $T_{\rm eff}$ the behaviour is less clear. Then, the exact difference between the $T_{\rm c}$ trends depends on the fundamental parameters of the stars and of their chemical patterns.

5.1. Solar-scaled or not: are the differences significant?

At first view, a difference of 0.01 dex in metallicity or 15 K in $T_{\rm eff}$ does not seem significant. For instance, a number of works show that giant planets form preferentially around metal-rich stars (e.g. Santos et al. 2004, 2005; Fischer & Valenti 2005), which is known as the giant planet–metallicity correlation. In these statistical works with hundreds of objects, an individual dispersion in [Fe/H] of 0.01 or 0.02 dex would not be significant. However, exoplanet host stars are a fossil record of planet formation, beyond the giant planet–metallicity correlation. Using a high-precision abundance analysis, Meléndez et al. (2009) found a lack of refractories in the atmosphere of the Sun when compared with the average abundances of 11 solar twins. The authors found a trend between the abundances and $T_{\rm c}$ of the different chemical species as a possible signature of rocky planet formation. They proposed that the refractory elements absent in the Sun's atmosphere were used to create rocky planets and the nuclei of giant planets. This idea was followed by a number of works in the literature (see e.g. Ramírez et al. 2010; Tucci Maia et al. 2014; SA15; SA16; SA17). The detection of this planetary chemical signature is a very challenging task, requiring a careful and detailed analysis of the data, as we explain below.

The complete $T_{\rm c}$ trend detected by Tucci Maia et al. (2014) for the stars of the binary system 16 Cyg, covers a range of only 0.04 dex between the maximum and minimum abundance values of 19 different chemical species (see their Fig. 3). We showed previously (Fig. 1) that a number of species show an abundance difference (new method − solar-scaled) larger than the ∼0.01 dex of the [Fe/H], reaching ∼0.03 dex in HAT-P-4 (e.g. Nd or Sm), with some elements showing even the opposite difference (e.g. C and O). Thus, it is clear that the inclusion or not of this effect

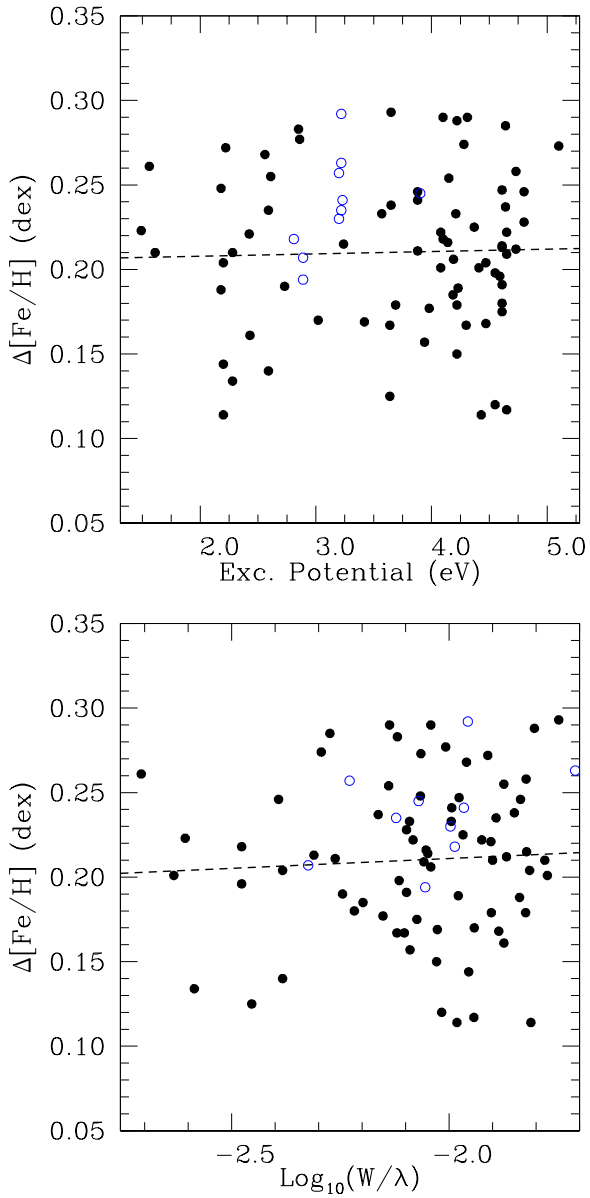

Fig. 3. Iron abundance vs. excitation potential (*upper panel*) and iron abundance vs. reduced EW (*lower panel*) for the star HAT-P-4, derived with non-solar-scaled opacities but applying the solution of the solar-scaled method. Filled and empty points correspond to Fe I and Fe II, respectively. The dashed line is a linear fit to the abundance values (see text for details).

will have an important impact on the detection of a possible T_c trend in objects such as the stars of the 16 Cyg binary system where the complete trend covers only 0.04 dex. This shows that the detection of a possible T_c trend (as a chemical signature of planet formation) requires the maximum achievable precision in both stellar parameters and abundances. In general, we can say that those high-precision studies whose results depend on the mutual comparison of different chemical species should use the non-solar-scaled method.

It is also notable that our Sun is considered a typical star in the context of the giant planet-metallicity correlation; however, the same Sun shows a clear T_c trend when compared with solar twins (Meléndez et al. 2009; Ramírez et al. 2010) using very high-precision abundances. This apparent dichotomy derives in part from the precision reached in these different works. It would be very difficult (if not impossible) to detect a slight T_c trend by applying only standard techniques (e.g. non-differential) rather than high-precision methods of stellar parameters derivation.

The search for a possible chemical signature of planet formation is not the only reason to pursue high-precison stellar parameters. Several examples in the literature show that a precise planetary characterization depends on the precise derivation of stellar parameters. For instance, Bedell et al. (2017) revised the stellar parameters of the host star Kepler-11 using a high-precision spectroscopic method and showed that the planet densities increased by between 20 and 95% per planet compared to previous works. Other examples correspond to the derivation of the planetary radius which depends on the stellar radius, which in turn is derived from the fundamental parameters $T_{\rm eff}$, log g, [Fe/H], and $v_{\rm micro}$ (see e.g. Johnson et al. 2017). Notably, the improved derivation of parameters allowed the detection of a gap in the radius distribution of small planets ($R < 2\ R_{\rm Earth}$; Fulton et al. 2017), showing the possible presence of two different populations of planets (rocky planets and Neptune-like planets). Thus, the importance of precise stellar parameters is evident. Also, we can consider the missing mass of refractory material in the atmosphere of the stars due to the planet formation process, estimated using the models of Chambers (2010). Using the solar-scaled results for the star HAT-P-4, we obtain $M_{\rm rock} = 7.2 \pm 0.4\ M_{\rm Earth}$, while using the non-solar-scaled values we derive $M_{\rm rock} = 8.6 \pm 0.4\ M_{\rm Earth}$, i.e. a 20% difference. This error could be avoided by using the new estimation of parameters. The need to reach the highest possible precision in these works is clear.

Following the previous considerations, we can summarize as follows. If we are working with a large sample of stars, for example trying only to detect a global difference in metallicity of ∼0.20 dex between two subgroups, then an individual dispersion of ∼0.01 dex does not seem significant. On the contrary, if we are trying to detect a relative difference in abundances of different species (e.g., a T_c trend) or the missing mass of refractory material due to the planet formation process, for example, then it is worthwhile to use the highest possible precision. It is also important to keep in mind that some chemical species show differences greater than that of [Fe/H]. We caution that the use of a lower precision will certainly tend to mask or smooth out the signal of any physical process, which requires a higher precision to be detected.

5.2. Bias in studies of many stars?

From Table 2 it is not clear that a single parameter determines the differences between the two methods, although $T_{\rm eff}$ seems to play a role. However, we can suppose that a group of stars in the solar neighborhood presents a chemical pattern quite similar to the solar one, while other stars have in general a non-solar-scaled pattern. Suppose that we obtain stellar parameters for all stars using the classical two-step method and the non-solar-scaled method. Those stars in the first group will show similar parameters derived with the two methods, given their approximately solar chemical pattern. However, the stars in the second group will present a difference in their parameters which gradually increases as stars present patterns farther and farther from solar. This would correspond to a possible small bias in the parameters, depending on the chemical composition of the stars considered. In addition, Castelli (2005a) has shown that the internal temperature distribution T versus log $\tau_{\rm Rosseland}$ of ATLAS9 and ATLAS12 model atmospheres differ with increasing $T_{\rm eff}$, adopting in principle the same abundance pattern in both cases,

leading us to consider that a possible small bias cannot be totally ruled out. We will address this important question in detail quantitatively in a next work.

6. Conclusion

We used non-solar-scaled opacities for a simultaneous derivation of stellar parameters and chemical abundances in a sample of solar-type main-sequence and evolved stars. To date, this is probably one of the most precise spectroscopic methods for determining stellar parameters. The difference in stellar parameters could amount to +26 K in $T_{\rm eff}$, 0.05 dex in log g, and 0.020 dex in [Fe/H], when using solar-scaled versus non-solar-scaled methods. We note that some chemical species could also show a variation greater than those of the [Fe/H] and varying from one species to another, obtaining a chemical pattern difference between the two methods. This means that $T_{\rm c}$ trends could also present a variation. The differences were derived using the full line-by-line differential technique, i.e., for the derivation of stellar parameters and of chemical abundances. We do not consider that the use of non-solar-scaled opacities should necessarily be mandatory, for example, in statistical studies with a large sample of stars. On the contrary, those high-precision studies whose results depend on the mutual comparison of different chemical species (such as a $T_{\rm c}$ trend) should preferably use the non-solar-scaled method. In these cases, when modelling the atmosphere of the stars, the four stellar parameters usually taken as ($T_{\rm eff}$, log g, [Fe/H], $v_{\rm micro}$) should in fact be taken as ($T_{\rm eff}$, log g, chemical pattern, $v_{\rm micro}$), which is conceptually closer to the real case.

Acknowledgements. M.F., F.M.L., and M.J.A. acknowledge the financial support from CONICET in the form of Post-Doctoral Fellowships. The authors also thank the referee for the comments that greatly improved the paper.

References

Adibekyan, V., Sousa, S., Santos, N., et al. 2012, A&A, 545, A32
Adibekyan, V., Figueira, P., Santos, N., et al. 2013, A&A, 554, A44
Adibekyan, V., González Hernández, J., Delgado Mena, E., et al. 2014, A&A, 564, L15
Adibekyan, V., Delgado Mena, E., Figueira, P., et al. 2016, A&A, 592, A87
Bedell, M., Meléndez, J., Bean, J., et al. 2014, AJ, 795, 23
Bedell, M., Bean, J., Meléndez, J., et al. 2017, ApJ, 839, 94
Bedell, M., Bean, J., Meléndez, J., et al. 2018, ApJ, 865, 68
Bonifacio, P., Spite, M., Cayrel, R., et al. 2009, A&A, 501, 519
Castelli, F. 2005a, Mem. Soc. Astron. It. Suppl., 8, 25
Castelli, F. 2005b, Mem. Soc. Astron. It. Suppl., 8, 34
Castelli, F., & Kurucz, R. L. 2003, Proc. IAU Symp., 210, A20
Castelli, F., Gratton, R. G., & Kurucz, R. 1997, A&A, 324, 432
Chambers, J. 2010, ApJ, 724, 92
Coelho, P. 2014, MNRAS, 440, 1027
Delgado Mena, E., Tsantaki, M., Adibekyan, V., et al. 2017, A&A, 606, A94
Desidera, S, Gratton, R., Scuderi, S., et al. 2004, A&A, 420, 683
Fischer, D., & Valenti, J. 2005, AJ, 622, 1102
Fischer, D., Anglada-Escude, G., Arriagada, P., et al. 2016, PASP, 128, 6001
Fulton, B., Petigura, E., Howard, A., et al. 2017, AJ, 154, 109
González Hernández, J., Israelian, G., Santos, N., et al. 2010, ApJ, 720, 1592
González Hernández, J., Delgado Mena, E., Sousa, S., et al. 2013, A&A, 552, A6
Johnson, J. A., Petigura, E., Fulton, B., et al. 2017, AJ, 154, 108
Kurucz, R. L. 1992, The Stellar Populations of Galaxies, IAU, Symp., 149, 225
Kurucz, R. L. 1993, ATLAS9 Stellar Atmosphere Programs and 2 km s^{-1} Grid, Kurucz CD-ROM No. 13 (Cambridge, MA: Smithsonian Astrophysical Observatory)
Kurucz, R., Bell, B. 1995, Atomic Line Data, Kurucz CD-ROM No. 23 (Cambridge, MA: Smithsonian Astrophysical Observatory)
Kurucz, R. L., Peytremann, E., & Avrett, E. H. 1974, Blanketed Model Atmospheres for Early-type Stars (Washington, DC: Smithsonian Institution, of Docs., Government Printing Office), 37
Lo Curto, G., Pepe, F., Avila, G., et al. 2015, The Messenger 162, 9
Lodders, K. 2003, AJ, 591, 1220
Martioli, E., Teeple, D., Manset, N., et al. 2012, Software and Cyberinfrastructure for Astronomy II, Proc. SPIE, 8451, 21
Mayor, M., & Queloz, D. 1995, Nature 378, 355
Meléndez, J., Asplund, M., Gustafsson, B., & Yong, D. 2009, AJ, 704, L66
Mucciarelli, A., Bellazzini, M., Ibata, R., et al. 2012, MNRAS, 426, 2889
Peytremann, E. 1974, A&A, 33, 203
Ramírez, I., Asplund, M., Baumann, P., Meléndez, J., & Bensby, T. 2010, A&A, 521, A33
Ramírez, I., Meléndez, J., Cornejo, D., Roederer, I., Fish, J. 2011, AJ, 740, 76
Saffe, C. 2011, RMxAA, 47, 3
Saffe, C., Flores, M., & Buccino, A. 2015, A&A, 582, A17
Saffe, C., Flores, M., Jaque Arancibia, M., et al. 2016, A&A, 588, A81
Saffe, C., Jofré, E., Martioli, E., et al. 2017, A&A, 604, L4
Santos, N. C., Israelian, G., & Mayor, M. 2004, A&A, 415, 1153
Santos, N. C., Israelian, G., Mayor, M., et al. 2005, A&A, 437, 1127
Sbordone, L., Bonifacio, P., Marconi, G., et al. 2005, A&A, 437, 905
Sousa, S., Santos, N., Mayor, M., et al. 2008, A&A, 487, 373
Sousa, S., Santos, N., Israelian, G., et al. 2011a, A&A, 533, A141
Sousa, S., Santos, N., Israelian, G., et al. 2011b, A&A, 526, A99
Sneden, C. 2016 ApJ, 184, 839
Tucci Maia, M., Meléndez, J., & Ramírez, I. 2014, ApJ, 790, L25
Wolszczan, A., & Frail, D. 1992, Nature 355, 145